scientific reports

Check for updates

OPEN

A novel role for colistin as an efflux pump inhibitor in multidrug-resistant *Klebsiella pneumoniae*

Rajnikant Sharma[1], Shekhar Yeshwante[1], Ngoc Minh Bui[1], Vincenzo Carbone[2], Leslie Hicks[3], Bruce E. Blough[4], Tony Velkov[5] & Gauri G. Rao[1]✉

Antimicrobial resistance (AMR) is a global challenge that demands new strategies to maintain the effectiveness of current treatments. AMR arises through various mechanisms, including overexpression of drug efflux pumps. The AcrAB-TolC efflux pump is used by Enterobacterales such as *Klebsiella pneumoniae* to expel antibiotics and overcome antimicrobial toxicity. Here we explored a novel secondary activity of colistin as an efflux pump inhibitor. Experiments were conducted to determine antimicrobial susceptibility, selection of a resistant mutant, assess the function of efflux machinery under various treatment conditions, and measure the inhibition of extrusion by colistin. Colistin augmented the efficacy of various antibiotics against resistant *K. pneumoniae* strains and reversed clinically relevant antibiotic resistance caused by *acrAB* overexpression. This effect was demonstrated via increased uptake of efflux pump substrates such as *N*-phenyl-1-napthylamine, ethidium bromide, and Hoechst dye in *K. pneumoniae* overexpressing the AcrAB efflux pump. Molecular docking models indicated that colistin likely binds to the transmembrane region of *K. pneumoniae* AcrB, further validating colistin's function as an efflux pump inhibitor at low concentrations. Scanning electron microscopy showed that sub-nephrotoxic concentrations of colistin had no effect on bacterial membrane integrity. These novel findings highlight the therapeutic potential of sub-nephrotoxic concentrations of colistin as an adjuvant to overcome efflux-mediated resistance in clinically problematic Enterobacterales *K. pneumoniae*.

Keywords Antimicrobial resistance, Colistin, Efflux pump, Enterobacterales, *Klebsiella pneumoniae*

The emergence of multi-drug resistant bacterial pathogens is a major global concern[1]. Gram-negative pathogens present a particular challenge due to their impermeable outer membranes and sparse new anti-Gram-negative drug approvals. The outer membrane hinders passage of environmental toxins, preventing them from crossing the cellular membrane or entering the periplasm, thereby protecting the bacterial cell. Even when some bacterial noxious compounds such as antibiotics do manage to enter the cell, bacterial efflux pumps promptly export them, reducing intracellular antibiotic concentrations. This survival mechanism allows resistant bacteria to persist when challenged with higher antibiotic concentrations[1–4]. Poly-specific drug efflux transporters play a dual role in antibiotic resistance by not only causing intrinsic resistance by reducing antibiotic concentrations within bacteria but also enabling the development of class-specific resistance. These resistance mechanisms often cooperate synergistically[5].

Klebsiella pneumoniae is a Gram-negative pathogen responsible for various nosocomial infections, and is particularly problematic in clinical practice due to multiple antibiotic resistance mechanisms. Among these, overexpression of efflux pumps results in resistance to clinically relevant antibiotics. These pumps are encoded by bacterial housekeeping genes and vary in substrate specificity, membrane topology, energy, and coupling mechanisms[6,7]. Based on these fundamental characteristics, five efflux pump families have been categorized that are widely distributed among *K. pneumoniae*. Among these, the resistance-nodulation-division (RND) family of pumps are particularly attractive targets for drug development. One such RND-family member is AcrAB-TolC -, previously characterized in *K. pneumoniae*[8] and a model pump in Enterobacterales for efflux pump-related studies[9]. This pump forms a tripartite complex of three proteins: TolC (an outer membrane protein channel), AcrB

[1]USC Alfred E. Mann School of Pharmacy and Pharmaceutical Sciences, University of Southern California, Los Angeles, CA, USA. [2]AgResearch, Grasslands Research Centre, Tennent Drive, Private Bag 11008, Palmerston North 4442, New Zealand. [3]Department of Chemistry, University of North Carolina at Chapel Hill, Chapel Hill, NC, USA. [4]Research Triangle Park, Durham, NC, USA. [5]Biomedicine Discovery Institute, Department of Pharmacology, Monash University, Clayton, VIC, Australia. ✉email: gaurirao@usc.edu

(an inner membrane pump protein), and AcrA (a periplasmic linker protein). AcrB, with its diverse substrate specificity, uses the proton motive force to actively expel various structurally dissimilar substrates, including several clinically relevant antibiotics, against their concentration gradient[10]. Some efflux pump substrates have been studied by co-crystallization at different locations of the efflux pump protein[11].

Any deletion or deactivation of a gene encoding a component of this efflux pump renders bacterial strains highly susceptible to the pump's substrates. However, overexpression of efflux pumps can induce low-level cross-resistance to beta-lactams and other antibiotics like quinolones and amphenicol[12]. Notably, there have been reports of increased dissemination of bacterial strains with active drug efflux mechanisms in hospitals, impacting the efflux of various antibiotics and other compounds[13–15]. Given the significance of efflux pumps in enabling bacteria to evade the killing effect of drugs, further research is warranted.

RND efflux pumps represent a promising target for discovering and developing novel antibacterial adjuvants. Notably, these pumps lack human homologs, making them ideal selective therapeutic targets[8,16–21]. Efflux pump inhibitors (EPIs) are therefore a promising and valid strategy in the fight against antibacterial resistance[7,22] enhancing antibiotic efficacy by increasing their intracellular concentrations and reducing the frequency of target-based resistance[23,24]. Four classes of EPIs have been identified, namely peptidomimetics[25] piperazines[26] pyridopyrimidines[27] and pyranopyrimidines[28]. However, none have been approved for clinical use due to toxicity[29].

Given this translational gap, we investigated the efflux inhibitory effects of the lipopeptide antibiotic colistin. To achieve this, we created knockout and overexpression strains of the *acrAB* efflux pump in *K. pneumoniae* ATCC43816. We then proceeded to evaluate and validate colistin's efflux inhibitory activity using these genetically-modified strains.

Results

Impact of *acrAB* deletion and overexpression on drug phenotypes in the presence and absence of colistin

The successful construction of an *acrAB* mutant strain (*K. pneumoniae* ATCC43816_ΔacrAB) (Fig. 1A) was confirmed using conventional methods (Fig. 1B) and RT-PCR (Fig. 1C). We then determined the MICs of various antibiotics (Table 1) for the wild-type strain, the *acrAB* knockout strain (*K. pneumoniae* ATCC43816_ΔacrAB), and the *acrAB* overexpressor strain (*K. pneumoniae* ATCC43816_ΔacrAB::pWKS_acrAB) (Table 1). Notably, the *acrAB* overexpressor showed a two-fold-higher MIC for tetracycline, a four-fold-higher MIC for cefoxitin, chloramphenicol, sulfamethoxazole, piperacillin, and minocycline, and a 16-fold-higher MIC for erythromycin compared with the isogenic *acrAB* knockout strain (Table 1). Interestingly, the MIC of colistin alone, was 1 mg/L for all strains.

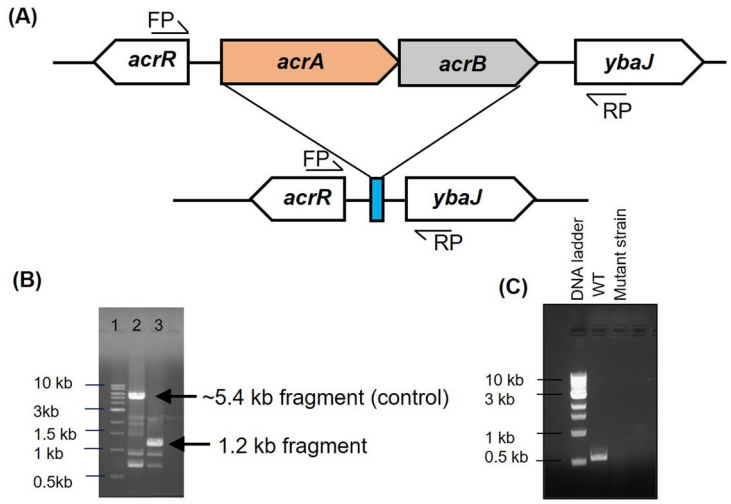

Fig. 1. Construction of *acrAB* efflux pump mutant strain (ATCC 43816_ΔacrAB). **(A)** Genetic deletion of *acrAB*: The *acrAB* gene was deleted in *Klebsiella pneumoniae* ATCC 43,816 using the FLP-FRT system. The process involves two steps: (1) a recombinant PCR product introduced an apramycin cassette flanked by FRT sites and 60 base pairs of upstream and downstream regions of *acrAB*. This cassette replaced the *acrAB* gene via homologous recombination; (2) FLP recombinase then removed the apramycin cassette between the adjacent FRT sites, leaving a scar (depicted as a light blue box). **(B)** Gel confirmation: Deletion was verified in the mutant strain using gel electrophoresis. Primer pairs (FP and RP) were used for PCR validation. The small arrows in part A indicate the approximate binding locations of these primers. Specifically, we amplified a ~ 5.4 kb fragment in the wild type (WT) strain and a ~ 1.2 kb fragment in the mutant strain. **(C)** Reverse-transcriptase PCR: To further confirm deletion of *acrAB*, we performed reverse-transcriptase PCR. The gene specific primers amplified the internal part of *acrAB*, which was detectable only in the WT strain. **Note: The** full length gel images (Fig. 1B, C) has been included in the supplementary material as supplementary Fig. 6B, & C.

Antibiotic	*K. pneumoniae*		
	ATCC43816	ATCC43816_ΔacrAB/pWKS130	ATCC43816_ΔacrAB::pWKS_acrAB
Ceftazidime	< 0.5	< 0.5	< 0.5
Cefazolin	1	2	2
Cefoxitin	1	1	**4 (4)**
Aztreonam	< 0.5	< 0.5	< 0.5
Meropenem	< 0.5	< 0.5	< 0.5
Gentamycin	< 0.5	< 0.5	< 0.5
Ciprofloxacin	< 0.5	< 0.5	< 0.5
Tigecycline	< 0.5	< 0.5	< 0.5
Chloramphenicol	**4**	**1**	**4 (4)**
Colistin sulfate	1	1	1
Tetracycline	**2**	**2**	**4 (2)**
Sulfamethoxazole	**64**	**32**	**128 (4)**
Piperacillin	**4**	**1**	**4 (4)**
Levofloxacin	< 0.5	< 0.5	< 0.5
Minocycline	**1**	**< 0.5**	**2 (4)**
Streptomycin	2	2	2
Erythromycin	**32**	**4**	**64 (16)**

Table 1. MIC results of antibiotics against ATCC43816 wild-type, knockout, and *acrAB* overexpressor.

Antibiotic	ATCC43816_ΔacrAB::pWKS_acrAB MIC (mg/L) (Fold change)	
	Without colistin	With colistin 0.5 mg/L
Chloramphenicol	8	**4 (2)**
Minocycline	4	**1 (4)**
Erythromycin	128	**64 (2)**
Sulfamethoxazole	16	16
Piperacillin	4	4
Meropenem	< 0.5	< 0.5
Cefoxitin	4	4
Tetracycline	4	4
Ciprofloxacin	< 0.5	< 0.5

Table 2. MIC results for antibiotics in the presence and absence of 0.5 mg/l colistin against ATCC43816 knockout strain overexpressing *acrAB* efflux pumps.

Subsequently, we determined the MICs of selected antibiotics in the presence of colistin (0.5 mg/L) against the *acrAB* expressor strain (Table 2). Notably, colistin reduced the MICs of minocycline (four-fold) and chloramphenicol (two-fold), both of which are known substrates of the AcrAB efflux pump. These findings suggest that colistin's potentiating effect on these antibiotics may be due to its inhibitory action against the RND pump protein.

Colistin-mediated Inhibition of N-phenyl-1-napthylamine (NPN) efflux via the AcrAB efflux protein

To assess colistin as an efflux pump inhibitor, we investigated the efflux of NPN in *K. pneumoniae* strains with and without *acrAB* expression in the presence of colistin (Fig. 2A, & B). NPN fluoresces strongly when bound to bacterial membranes. We initiated NPN efflux by adding glucose at 3 min to *K. pneumoniae* cells either lacking (Fig. 2A) or expressing *acrAB* (Fig. 2B) treated with CCCP loaded with NPN. Colistin was introduced 3 min after the addition of glucose, coinciding with the NPN fluorescence in *acrAB*-expressing cells caused by steady efflux activity. Interestingly, different colistin concentrations led to dose-dependent increases in NPN fluorescence in cells expressing *acrAB* (Fig. 2B). Even the modest decrease in NPN fluorescence observed in the *acrAB* knockout strain was enhanced with the addition of colistin (Fig. 2A), indicating colistin's efflux inhibitory activity. Notably, NPN fluorescence in *acrAB*-expressing cells reached pre-efflux levels (i.e., fluorescence levels prior to initiating efflux) within 3- and 4-minutes following addition of 100 and 50 µM colistin, respectively (Fig. 2B). In the case of the *acrAB* knockout strain, all colistin concentrations except 5 µM resulted in pre-efflux-level NPN fluorescence within 2 min after the addition of colistin (Fig. 2A). These findings collectively demonstrate that both knockout and overexpressor strains showed colistin-mediated inhibition of NPN efflux, albeit with slight differences.

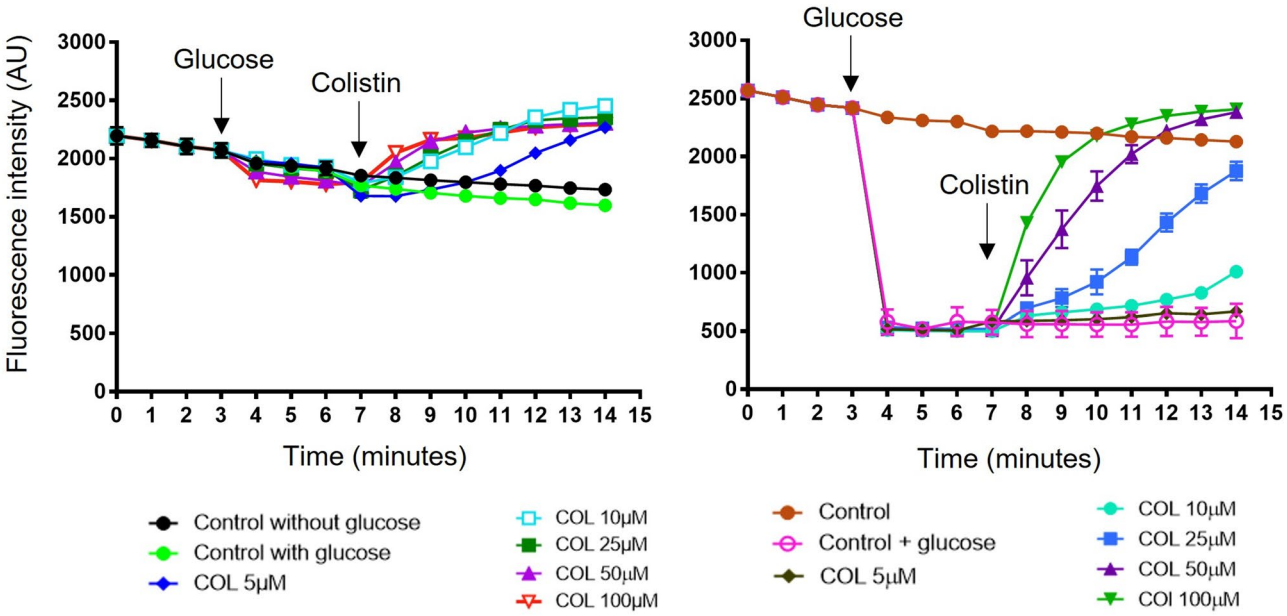

Fig. 2. Inhibition of NPN efflux by colistin. (**A**) NPN efflux in *K. pneumoniae* ATCC43816 ΔacrAB cells: Initially, *K. pneumoniae* ATCC43816 with *acrAB* knockout were exposed to 100 μM CCCP and preloaded with 9 μM NPN for 10 min. NPN extrusion was initiated by adding glucose alone (depicted as green circles). Subsequently, colistin was added 3 min after the start of NPN efflux, resulting in final concentrations ranging from 5 to 100 μM. The decay of NPN fluorescence in the presence of glucose was compared to the control (no glucose, represented as black circles). **(B)** NPN extrusion in *K. pneumoniae* ATCC43816 overexpressing *acrAB*. NPN extrusion was observed in cells overexpressing the AcrAB efflux pump. Glucose, either alone or in combination with different colistin concentrations, was added to CCCP-treated, NPN-loaded cells. Colistin (5-100 μM) inhibited extrusion of NPN in a dose-dependent manner. Notably, at higher colistin (COL) concentrations (100 μM), NPN fluorescence increased significantly, indicating complete inhibition of AcrAB-mediated NPN efflux. The units are arbitrary (AU).

We next tested the hypothesis that the positive charge of colistin might displace outer membrane-bound cations and potentially increase NPN fluorescence. To do so, we examined the effect of EDTA (known to disrupt outer membrane integrity) by adding it 3 min after glucose addition, allowing real-time monitoring of its impact on NPN efflux. Surprisingly, EDTA at concentrations from 10 to 100 μM did not increase NPN fluorescence in any strain (Supplementary Fig. 1 A & B), suggesting that chelation of outer membrane cations does not play a role in colistin-mediated NPN fluorescence enhancement.

To explore the effect of membrane lysis on NPN efflux, we used the anionic detergent sodium dodecyl sulfate (SDS). Adding SDS three minutes after the addition of glucose revealed an immediate increase in NPN fluorescence, surpassing the pre-efflux fluorescence in the *acrAB*-knockout strain (Supplementary Fig. 2 A) and indicating that SDS-mediated cell lysis contributes to the increase in NPN fluorescence. Interestingly, the AcrAB overexpressor strain also exhibited an instant increase in NPN fluorescence upon addition of SDS, irrespective of its concentration (Supplemental Fig. 2B), although the fluorescence did not exceed pre-efflux levels. The fluorescence of the NPN and SDS solution without bacterial cells was measured as a negative control and did not show any significant increase in the fluorescence compared to the blank buffer solution.

To investigate whether colistin has a detergent-like effect on colistin-sensitive bacterial cells, we employed a colistin-resistant strain (BRKP67 with colistin MIC of 8 mg/L) and conducted an NPN efflux assay. A commercially available efflux pump inhibitor PaβN was used as a positive control. After incubating BRKP67 bacterial cells with NPN and varying concentrations of colistin (from 25 μM to 100 μM) for 30 min, we observed a 3.7- to 4.0-fold increase in NPN fluorescence compared with the negative control. Similarly, PaβN treatment resulted in a 1.5- to 2.8-fold increase in NPN fluorescence relative to the untreated control (Supplemental Fig. 3 A).

Assessing efflux activity using the Hoechst H33342 accumulation assay

EtBr and H33342 (bisbenzimide) are commonly used fluorescent probes that fluoresce when bound to DNA. The increased fluorescence intensity corresponds to greater accumulation of the H33342 dye within the cell. During the assay, H33342 added to the extracellular environment diffuses into bacteria and fluorescence intensity negatively correlates with efflux activity. As a positive control, PAβN demonstrated increased fluorescence intensity relative to untreated cells. In the H33342 fluorescence assay, *K. pneumoniae* expressing the AcrAB efflux pump exhibited a greater than two-fold increase in fluorescence intensity after treatment with different concentrations of colistin compared with untreated cells (Fig. 3A). Similar results were observed with the colistin-resistant strain BRKP67 (colistin MIC 8 mg/L) (Supplemental Fig. 3B).

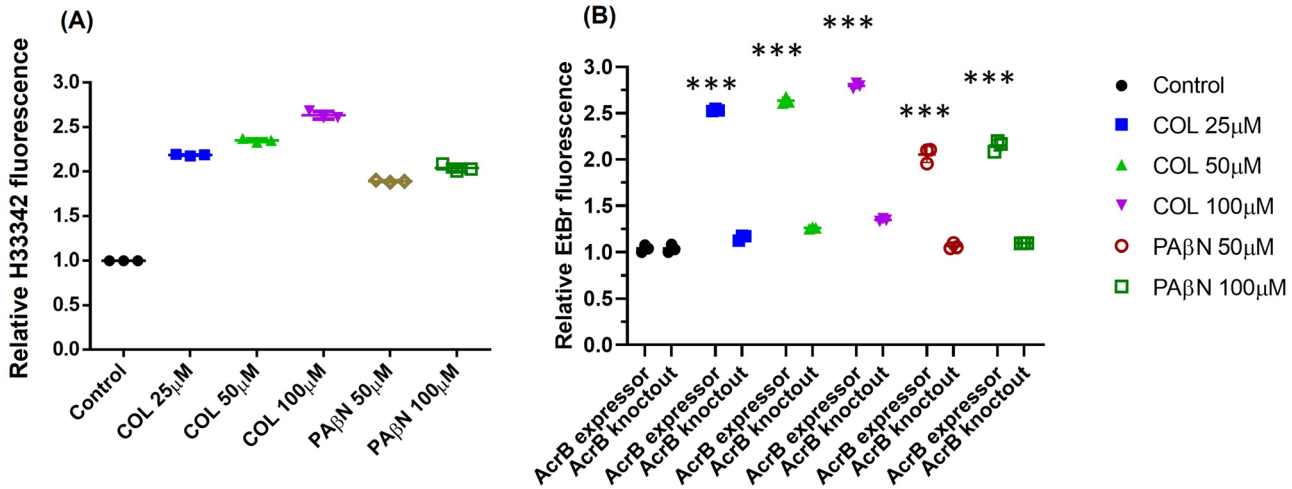

Fig. 3. Effect of colistin on Hoechst H33342 accumulation and ethidium bromide (EtBr) efflux. (**A**) Hoechst accumulation assay: Fluorescence of Hoechst dye inside cells was assessed to determine the impact of colistin. Hoechst accumulation in *K. pneumoniae* ATCC43816 overexpressing *acrAB* efflux pump was quantified at varying colistin concentrations. Colistin increased fluorescence intensity. **(B)** Efflux assay for EtBr: Efflux assays were performed using *K. pneumoniae* ATCC43816 overexpressing *acrAB* and *acrAB* knockout strains. EtBr accumulation was significantly higher in bacterial cells expressing *acrAB* efflux pumps compared with the control strain not expressing efflux pumps following colistin treatment. This suggests that colistin inhibits AcrAB efflux activity, leading to enhanced EtBr accumulation. Each data point represents a biological replicate, and all values are means ± SD ($n = 3$), normalized to the colistin-free control. Statistical analysis was conducted using 2-way ANOVA followed by a post-hoc Sidak test to determine the significant differences in accumulation fluorescence between AcrB mutant and expressor strains after treatment with different concentrations of colistin. ***, $P < 0.001$.

For the EtBr efflux assay, we de-energized bacteria by treating them with CCCP. Next, we preloaded bacteria with EtBr and added glucose during the assay to reenergize the cells and initiate efflux. As expected, this led to a loss of EtBr fluorescence. Specifically, *K. pneumoniae* ATCC43816 cells expressing AcrAB efflux pump showed a > 2.5-fold increase in fluorescence intensity after treatment with different colistin concentrations compared with untreated cells (Fig. 3B). However, the *K. pneumoniae* ATCC43816 *acrAB* knockout strain did not exhibit more than a 1.3-fold change in fluorescence intensity, even at the highest colistin concentration (Fig. 3B). All colistin concentrations evaluated in AcrB expressor strain showed a significant increase ($p < 0.0001$) in the fluorescence compared to the mutant strain. We also performed the EtBr efflux assay with the BRKP67 isolate, observing a more than two-fold increase in EtBr fluorescence with different colistin concentrations compared with the untreated control (Supplemental Fig. 3 C).

Enhanced intracellular accumulation of ciprofloxacin induced by colistin

To evaluate colistin as an efflux pump inhibitor, we assessed accumulation of ciprofloxacin, (Fig. 4A) an AcrAB pump substrate, using an LC/MS-based assay. Initially, *K. pneumoniae* lacking or expressing *acrAB* were treated with colistin to inhibit bacterial efflux activity. Subsequently, bacteria were loaded with ciprofloxacin and, after lysing bacterial cells, intracellular ciprofloxacin concentrations were quantified. The addition of 25 or 50 μM colistin resulted in a ~ 2-fold increase in intracellular ciprofloxacin concentrations in both wild-type and *acrAB*-knockout strains (Fig. 4B). Interestingly, the AcrAB overexpressor strain exhibited a significant 5.3- or 4.1-fold increase in intracellular ciprofloxacin concentration with 25 or 50 μM colistin, respectively, over 10 min (Fig. 4B).

Colistin diminishes the frequency of chloramphenicol-resistant mutant selection

Observations revealed that the same concentration of chloramphenicol resulted in fewer mutant isolations when used in combination with colistin compared with chloramphenicol alone at equivalent concentrations. Specifically, chloramphenicol combined with 0.125, 0.25, and 0.5 mg/L colistin exhibited a reduced mutation selection frequency compared with chloramphenicol alone at the same concentrations (Table 3). Interestingly, none of the chloramphenicol concentrations in combination with 1 mg/L colistin yielded any mutations (Table 3).

Impact of colistin on bacterial cellular morphology

Morphology of *K. pneumoniae* ATCC43816 was compared after treatment with various colistin concentrations and controls (Fig. 5A, A1) by SEM. While treatment with 12.5 μM colistin did not result in significant morphological alterations in *K. pneumoniae* (Fig. 5B & B1), the higher colistin concentrations of 25 and 50 μM resulted in minor membrane blebbing (Fig. 5C, C1 & D, D1).

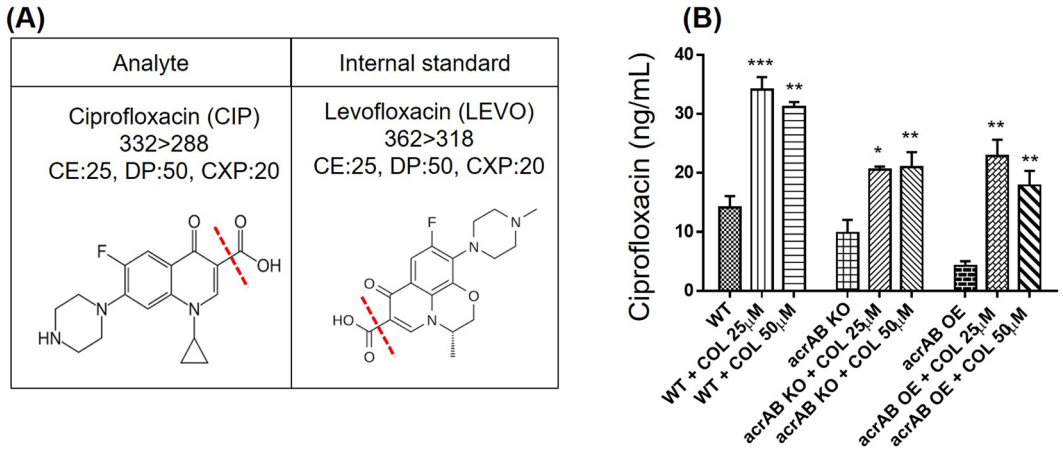

Fig. 4. Determination of intracellular ciprofloxacin concentrations using LC/MS. Ciprofloxacin (30 ng/mL) accumulation in *K. pneumoniae* ATCC43816 wild type (WT), *acrAB* knockout (KO), and *acrAB* efflux pump overexpressor (OE) strains for 10 min was measured using an LC/MS-based assay. All values shown are means ± SD ($n = 3$). **(A)** Analyte and internal standard structures: Detection parameters, including multiple reaction monitoring (MRM) transitions, were optimized for accurate quantification. **(B)** Intracellular ciprofloxacin concentration: Intracellular ciprofloxacin levels were compared in *K. pneumoniae* WT, *acrAB* efflux pump knockout (KO), and *acrAB* overexpressor (OE) strains, both with and without colistin. Statistical significance was determined using Student's *t*-test ($p < 0.05$).

Antibiotic combinations	Mutation selection frequency			
	0.5 mg/L CHL	1 mg/L CHL	2 mg/L CHL	4 mg/L CHL
Without colistin	1.017	0.908	0.867	3.2×10^{-5}
With colistin 0.125 mg/L	0.700	0.638	0.367	1.7×10^{-5}
With colistin 0.25 mg/L	0.089	3×10^{-3}	7×10^{-4}	2×10^{-6}
With colistin 0.5 mg/L	1×10^{-3}	5×10^{-4}	7×10^{-6}	3×10^{-7}
With colistin 1 mg/L	0.00	0.00	0.00	0.00

Table 3. Frequency of selection of Chloramphenicol (CHL)-resistant mutants in *K. pneumoniae* ATCC43816 *acrAB* overexpressor in the presence and absence of colistin.

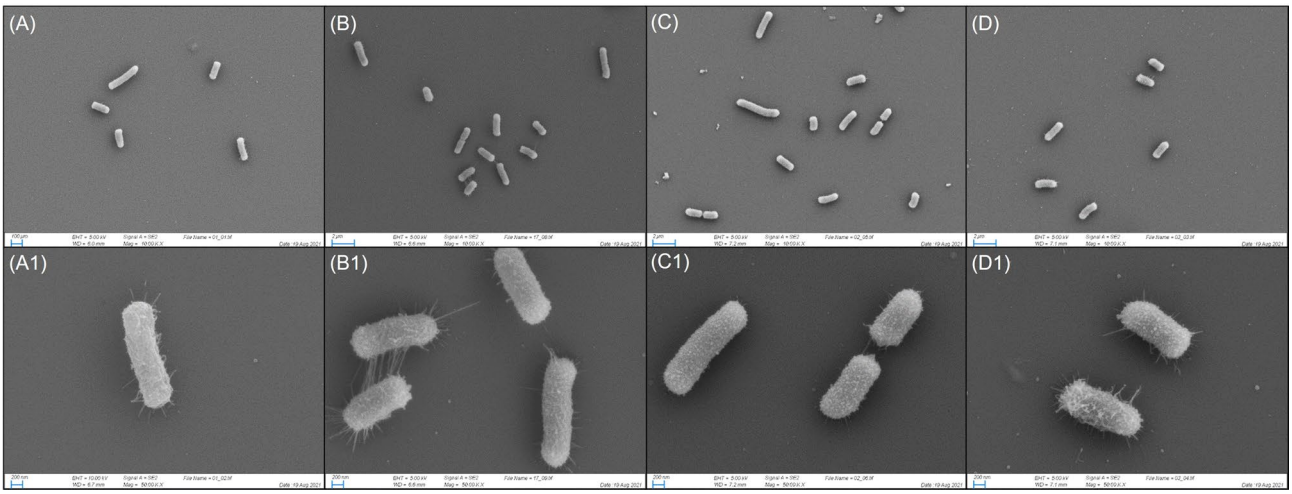

Fig. 5. SEM images of *K. pneumoniae* ATCC43816 after treatment with 12.5 μM (**B**, **B1**), 25 μM (**C**, **C1**), and 50 μM (**D**, **D1**) for 30 min. Control conditions are shown in (**A**, **A1**). Images A, B, C, and D are at 10,000x magnification, while A1, B1, C1, and D1 are at 50,000x magnification.

Colistin high concentrations increased the membrane potential

At high concentrations, colistin increased the membrane potential. The rise in cellular fluorescence at these concentrations indicates the movement of the charge specific dye, $DiBAC_4(3)$ across the bacterial membrane. Colistin at low concentrations (up to 1μM) did not affect the bacterial membrane potential (Supplemental Fig. 4).

Exploring the interaction between colistin and AcrB: docking insights

The crystal structure of membrane transporter protein AcrB (PDB code 4DX5) was selected for docking due to its high resolution (1.9 Å) and co-crystallization with multiple substrates, including minocycline and doxorubicin[30]. Inhibitors have been shown to exhibit similar amino acid binding as observed in 4DX5, supporting its use as a model for further computational investigations. The AcrB binding site consists mainly of hydrophobic amino acids, along with some ionized and polar residues, and amino acid diversity is essential for AcrB substrate and/or inhibitor binding[31]. We compared docking of PAβN (used as a positive control) with colistin at the LMU and MIY binding sites. At the LMU binding site, both PAβN and colistin interacted with Phe628, Phe617, Phe136, Met575, and Met573, with docking scores of −6.47 and − 10.34, respectively (Fig. 6A & C). At the MIY binding site, both PAβN and colistin interacted with Phe610, Phe628, Phe136, and Phe178, with docking scores of −8.32 and − 14.05, respectively (Fig. 6B & D).

Colistin showed binding affinity for AcrB

Molecular docking clearly indicates an apparent affinity between colistin and the AcrB protein. To support these findings, we used isothermal calorimetry (ITC) to demonstrate the binding affinity between colistin and AcrB. The purified, detergent-solubilized AcrB was titrated with colistin, and calorimetric signals were recorded. The titration profile showed gradually decreasing peak lengths after each injection, indicating saturation of the colistin binding site on AcrB. A single-site curve fitting model ($n = 1$) was used to determine the apparent K_d value of 0.32 μM for colistin (Supplemental Fig. 5).

Discussion

Bacterial efflux pumps play a critical role in both intrinsic and acquired antibiotic resistance. By overexpressing chromosomally encoded resistant determinants, bacteria can evade the effects of antibiotics[32]. Notably, certain antibiotics, like meropenem, exhibit pharmacodynamic killing activity against sensitive bacterial strains in the absence of efflux pump upregulation. Therefore, increasing intracellular concentration of these efflux substrates would be a very effective strategy to counteract multidrug resistance. Inhibiting efflux pumps can enhance antibiotic efficacy and improve clinical outcomes. Effective efflux pump inhibitors should enhance sensitivity to clinically-relevant antibiotics, possess favorable pharmacodynamic properties, and be non-toxic to human cells[33].

Here we investigated colistin's inhibitory effect on the RND family efflux pump AcrAB in Gram-negative bacteria, specifically *K. pneumoniae*. At higher concentrations, colistin destabilizes the bacterial outer membrane through electrostatic interactions and cationic displacement of liposaccharides, leading to cellular leakage and eventual cell death. Interestingly, at lower concentrations, colistin inhibited efflux pump activity, possibly by increasing membrane fluidity without significant disruption of phospholipids[34].

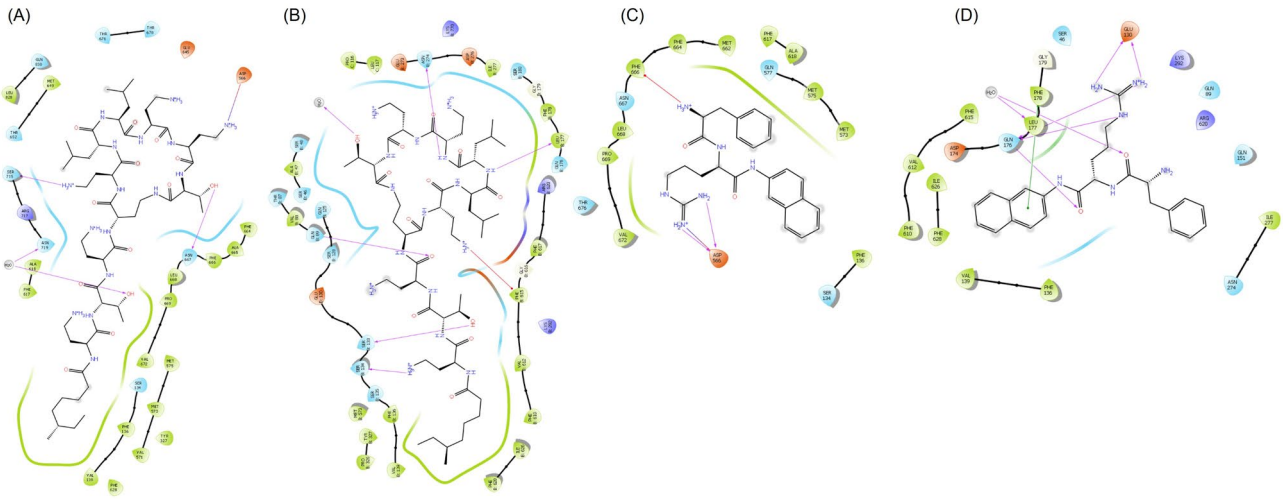

Fig. 6. Molecular docking of multidrug transporter AcrB (PDB code 4DX5) with PAβN and colistin. Molecular docking studies were performed to investigate interactions between multidrug transporter AcrB and two compounds, PAβN and colistin. These findings provide insights into the potential binding models of these compounds with AcrB. The top ranked pose for colistin was observed at the LMU (**A**) MIY binding site (**B**) of 4DX5. **PaβN docking**: The second ranked pose for PAβN was docked into the LMU-binding site (**C**) and the fourth ranked pose for PaβN was docked into the MIY-binding site of AcrB (4DX5) (**D**).

We demonstrated that sub-inhibitory concentrations of colistin enhance the effectiveness of antimicrobial agents. This increased antimicrobial activity was particularly notable in antibiotics whose resistance mechanisms are associated with efflux pumps and/or reduced membrane permeability (Table 2). Synergy between colistin and chloramphenicol has been reported at clinically-relevant concentrations against *K. pneumoniae*[35]. Additionally, studies involving colistin, similar peptides, and carbapenems in imipenem-resistant *P. aeruginosa* strains show synergistic effects[36]. Notably, increased expression of efflux pumps by MDR bacteria increases the frequency of spontaneous mutations[37] or facilitates the acquisition of plasmids[38] suggesting that efflux inhibitors may have potential to suppress the evolution of resistance across various combinations of antibiotics and pathogens. In this study, a sub-MIC concentration of colistin combined with chloramphenicol 4 mg/L showed ~ 100-fold reduction in the emergence of resistant mutant populations (Table 3). Other studies have also demonstrated that using an efflux pump inhibitor can prevent the emergence of resistance[39,40].

We used several assays to confirm colistin's efflux inhibitory activity against AcrAB efflux pumps, including measuring ethidium bromide efflux, accumulation of Hoechst dye, NPN fluorescence, and measuring intracellular ciprofloxacin concentrations using an LC/MS-based assay in the presence of colistin. The accumulation of fluorescent probes in bacterial cells after adding colistin indicated its efflux inhibitory effect. Additionally, the NPN efflux assay (Fig. 2) revealed concentration-dependent inhibition by colistin, with complete NPN efflux inhibition at 50 µM and 100 µM compared to a lower NPN accumulation at 10 µM and 25 µM. To confirm efflux inhibition and exclude membrane permeabilization by colistin, we performed EDTA- and SDS-based assays and, as expected, the addition of EDTA, an ion chelator that destabilizes the bacterial cell membrane, did not result in NPN accumulation. The increased NPN accumulation caused by colistin confirms that it exerts its effect without disrupting the membrane. The addition of SDS, an anionic detergent, resulted in a sharp but concentration-independent increase in NPN fluorescence, likely due to outer membrane disruption by SDS. However, colistin does not dissolve the outer bacterial membrane, as shown by SEM images, and increases NPN fluorescence in a concentration-dependent manner further supporting colistin's efflux inhibitory activity. Colistin exhibited similar activity to the well-known efflux pump inhibitor PaβN. However, at higher concentrations, colistin led to greater accumulation of Hoechst H33342 and EtBr (Fig. 3), with the minimal increases in EtBr accumulation seen in *acrAB* knockout with both colistin and PaβN further confirming colistin's efflux inhibitory properties. A similar concentration-dependent increase in NPN fluorescence was observed in *E. coli* overexpressing AcrAB-TolC when treated with the EPI molecule MC-207,110 [25]. Furthermore, quantitative LC/MS revealed that colistin treatment increased the accumulation of the substrate ciprofloxacin, leading to higher intracellular ciprofloxacin levels. To further validate colistin's role in inhibiting efflux activity, membrane depolarization and binding affinity assays were performed. The depolarization assay demonstrated that at higher concentrations colistin functions as a membrane depolarizer. Specifically, it disrupts the bacterial membrane by interacting with lipid A in the lipopolysaccharide layer, increasing membrane permeability. This allows greater uptake of the charge-specific dye, DiBAC4(3), resulting in enhanced fluorescence. However, at low concentrations, it functions as an efflux pump inhibitor by directly interacting with the AcrB protein, as shown by the ITC experiment (Supplemental Fig. 5). These findings collectively suggest that, beyond its antibacterial effects associated with lipopolysaccharide binding and outer membrane disruption, colistin can also inhibit efflux pumps.

Colistin has several advantages over other existing drugs when used as an efflux pump inhibitor. Although colistin can be nephrotoxic, prolonged intravenous administration at therapeutic concentrations (typically 2.5 to 5 mg/kg/day on average) does not elevate baseline serum creatinine levels in patients without pre-existing kidney issues[41]. Dose stratification based on mg/kg/day of ideal body weight (IBW) increased the risk of nephrotoxicity at higher doses, with nephrotoxicity occurring in 54.5% of patients at doses below 3 mg/kg/day, 63.23% at doses between 3 and 5 mg/kg/day, and 65% at doses exceeding 5 mg/kg/day[42]. Pogue et al. also reported dose-dependent colistin-associated nephrotoxicity, reaching 69% at doses of ≥ 5 mg/kg/day[43]. Furthermore, nephrotoxicity correlates with total dose and duration of therapy, with a four-fold increased risk observed in patients receiving treatment for more than 14 days[44–46]. Based on colistin clinical pharmacokinetics and toxicodynamic data, the risk of nephrotoxicity increased in patients with colistin plasma exposure exceeding 2.5 mg/L (average steady state concentration > 2 mg/L) and in patients with creatine clearance (CL_{Cr}) greater than 80 mL/min[47–51]. Importantly, colistin-induced nephrotoxicity is reversible upon discontinuation of therapy[44,52]. Therefore, using colistin at lower concentrations, well below therapeutic levels, could mitigate toxicity and enhance safety.

As colistin is an FDA-approved antibiotic with a well-documented pharmacokinetic profile, dosing can be tailored to individuals and combined with other antibiotics. Combining colistin with AcrAB-ToIC efflux pump substrates such as chloramphenicol, minocycline, and erythromycin could enhance their intracellular concentrations, rendering them more effective against ESKAPE pathogens[53]. In a clinical trial involving 53 cystic fibrosis patients with chronic pulmonary infections caused by MDR *P. aeruginosa*, colistin combined with an antipseudomonal agent (such as azlocillin, piperacillin, aztreonam, ceftazidime, imipenem, or ciprofloxacin) was more effective than using colistin alone[54]. Additionally, an in vitro study of two MDR *P. aeruginosa* strains demonstrated synergy between colistin and ceftazidime[55]. Furthermore, the combination of colistin, rifampin, and amikacin exhibited synergistic effects in vitro and successfully treated an immunosuppressed patient with multiple abscesses in the lungs, perineum, and gluteus caused by MDR *P. aeruginosa*[56].

In summary, we propose that colistin, when administered at low levels (sub-therapeutic concentrations), specifically inhibits activity of the AcrAB efflux pump. However, high colistin concentrations in efflux-proficient backgrounds and low concentrations in efflux-deficient backgrounds can result in membrane destabilization (Fig. 7). In addition to their use in combination with antibacterial agents, efflux pump inhibitors (EPIs) may also serve as valuable tools for studying the contribution and prevalence of efflux in bacterial virulence and intrinsic and acquired resistance to multiple antibiotics. A comprehensive future study of other efflux pumps and bacterial strains could pave the way for a sensor to identify efflux-mediated resistance.

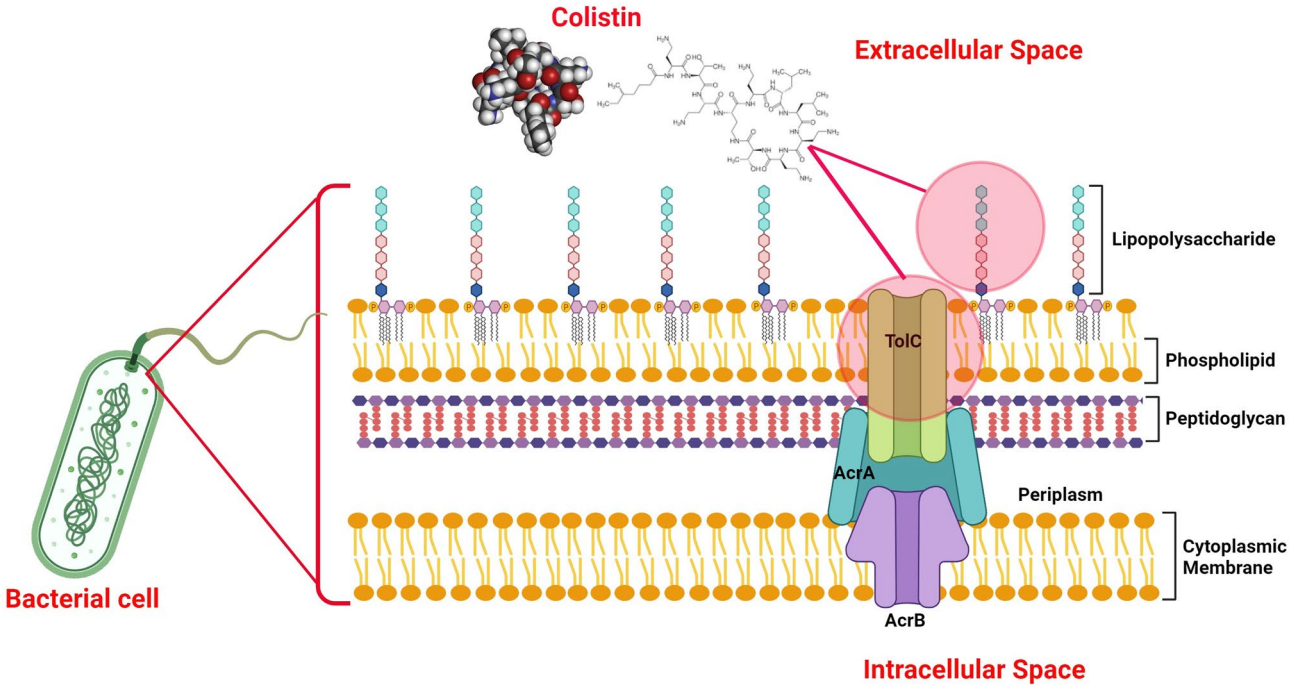

Fig. 7. Dual mechanism action of colistin in the bacterial cells. At lower concentrations colistin acts as efflux pump inhibitor in combination with efflux pump substrates. At higher concentrations colistin can disrupt the bacterial membrane by attaching to the lipid A of the lipopolysaccharide, attached to outer bacterial membrane.

Methods

Bacterial strains and plasmids

All bacterial strains and plasmids are described in Supplementary Table 1. *K. pneumoniae* ATCC43816 and *Escherichia coli* cells were grown in Luria-Bertani (LB) medium (Difco, Becton Dickinson, Franklin Lakes, NJ, USA) with constant shaking at 37 °C. Whenever required, growth media were supplemented with kanamycin, hygromycin, and apramycin (Sigma Aldrich, St. Louis, MO, USA) to a final concentration of 50 mg/L kanamycin and apramycin and 100 mg/L hygromycin.

In vitro antimicrobial susceptibility assay

MICs of various antibiotics and ethidium bromide (EtBr) were determined using the broth micro-dilution method in 96-well plates containing cation-adjusted Mueller Hinton broth (MHB) medium (Difco) as per Clinical & Laboratory Standards Institute (CLSI) guidelines[57].

Generation of *acrAB*-mutant and -overexpressing *K. pneumoniae* ATCC43816

The efflux pump gene knockout strains were constructed by homologous recombination using the λ-red knockout system as described previously[58]. Briefly, knockout cassettes were constructed using PCR primers (Supplementary Table 1) containing the 60 bp regions located upstream and downstream relative to efflux pump genes on the 5′ end of each primer; consensus sites were used to amplify *aac(3)IV* (apramycin cassette) and the flanking FRT sites from plasmid pIJ773 on the 3′ ends[59]. PCR amplification was performed using pIJ773 as a template to create the knockout cassette. 1000 ng of the knockout cassette was electroporated into *K. pneumoniae* ATCC43816 bearing pACBSR-Hyg (hygromycin resistant, containing the λ-red system used to facilitate homologous recombination between the knockout cassette and the target genes). Super Optimal broth with Catabolite repression (SOC) medium (Thermo Fisher Scientific, Waltham, MA, USA) supplemented with 100 mM arabinose (Sigma-Aldrich, USA) was used to grow bacterial cell transformants. Bacterial mutants were selected on LB agar plates supplemented with 50 mg/L apramycin. Correct insertion of knockout cassettes was confirmed via PCR using primers described in Supplementary Table 1. The colonies identified for correct insertion were serially passaged on LB plates containing apramycin for several days until they became sensitive to hygromycin, indicating loss of pACBSR-Hyg. Knockout cassettes in mutants were replaced by transforming them with pFLP-Hyg expressing FLP recombinase. The transformants were selected on low-salt LB agar plates with hygromycin. To facilitate excision of *aac(3)IV* (apramycin cassette) through homologous recombination between the two flanking FRT sites, FLP recombinase was induced by streaking 16 to 20 colonies onto an LB plate and heat-shocked at 43 °C and incubated overnight. The following day, all replicates from the incubated plates were streaked onto to a pair of LB and LB with apramycin plates to screen for loss of *aac(3)IV.* Apramycin-sensitive replicates were serially passaged onto LB plates at 37℃ until they had also regained hygromycin sensitivity, indicating loss of pFLP-Hyg. DNA was extracted from apramycin- and hygromycin-sensitive

colonies for PCR amplification and sequencing of the affected chromosomal gene to confirm knockout. Once the knockout was confirmed, the strain was designated *K. pneumoniae* ATCC43816_ΔacrAB.

For construction of the *K. pneumoniae* strain overexpressing *acrAB*, a 4362 bp *acrAB* fragment was amplified from the genomic DNA of *K. pneumoniae* ATCC43816 and cloned into pWKS130 plasmid between ApaI and XbaI restriction sites. The presence of the *acrAB* fragment was verified by direct sequencing of the recombinant plasmid and restriction digestion of the recombinant plasmid pWKS_acrAB. The recombinant plasmid pWKS_acrAB was then transformed into the knockout strain ATCC43816_ΔacrAB to create an overexpressor (ATCC43816_ΔacrAB ::pWKS_acrAB).

Reverse-transcriptase PCR

Total RNA was isolated from actively growing *K. pneumoniae* ATCC43816_ΔacrAB and ATCC43816_ΔacrAB::pWKS_acrAB cells using TRIzol reagent (Invitrogen, Thermo Fisher Scientific), and cDNA was synthesized using M-MLV reverse transcriptase enzyme (New England Biolabs, Ipswich, MA, USA) as per the manufacturer's instructions. cDNA was used as a template for amplification of the internal region of *acrAB* with gene-specific primers (Supplementary Table 1).

NPN N-phenyl-1-naphthylamine (NPN) and EtBr (ethidium bromide) fluorescence efflux assays

NPN is a substrate of RND efflux pumps[60] and efflux of NPN from live bacterial cells was assayed as described by Lomovskaya et al.[25]. Briefly, *K. pneumoniae* ATCC43816_ΔacrAB::pWKS130 and ATCC43816_ΔacrAB::pWKS_acrAB were cultured in MHB until reaching an optical density at 600 nm (OD_{600}) of ~ 1. Cells were then washed and resuspended in buffer A (50 mM K_2HPO_4, 1 mM $MgSO_4$, pH 7.0). The cell suspension was treated with 100 µM CCCP (carbonylcyanide *m*-chlorophenylhydrazone), washed, and then loaded with NPN at 9 µM for 15 min. NPN efflux was initiated with the addition of 0.4% glucose, and the decay in fluorescence was recorded. The fluorescence intensity was measured using excitation and emission wavelengths of 340 nm and 410 nm, respectively. After initiation of NPN efflux, different concentrations of colistin (ranging from 5 to 100 µM) were added to block NPN efflux. Phenyl-arginine-β-naphthylamide (PAβN) was used as a positive control.

EtBr efflux was assayed using a previously described method with some modifications[61]. Briefly, overnight cultures of genetically-modified *K. pneumoniae* ATCC43816 (ΔacrAB::pWKS130 and ΔacrAB::pWKS_acrAB) were used to inoculate fresh LB broth. The culture was then incubated at 37℃ to reach an OD_{600} of 0.45–0.60 corresponding to mid-exponential phase. Cells were harvested by centrifugation and re-suspended in 20 mM potassium phosphate buffer (pH 7.0) to achieve an OD_{600} of 0.2. Re-suspended cells were preloaded by incubating them with 100 µM CCCP (a protonophore) and 10 µg/mL EtBr for 30 min at room temperature. Cells were harvested by centrifugation and re-suspended in 20 mM potassium phosphate buffer to achieve to an OD_{600} of 0.1. Preloaded cells were added to a clear-bottom black 96-well plate containing varying concentrations of colistin, resulting in a final volume of 195 µL. EtBr fluorescence was measured at 37℃, with excitation and emission wavelengths set at 544 nm and 590 nm, respectively. The fluorescence of EtBr was measured at 1-minute intervals over 31 min using a spectrophotometer (Spectramax M2e, Molecular Devices, San Jose, CA, USA). After 5 measurements, 5 µL of glucose solution was added to each well to reach a final concentration of 25 mM. The experiment was repeated three times, and a graph depicting relative fluorescence over time elapsed was plotted.

Hoechst dye accumulation assay

Hoechst H33342 fluorescence served as an indicator of efflux activity as described previously[62]. An overnight culture of *K. pneumoniae* ATCC43816_ΔacrAB::pWKS_acrAB was used to inoculate fresh MHB and incubated at 37℃ until reaching an OD_{600} of 0.45–0.60, corresponding to mid-exponential phase. Cells were harvested by centrifugation and re-suspended in phosphate-buffered saline to achieve an OD_{600} of 0.1. These re-suspended cells were then added to a clear-bottom black 96-well plate containing varying concentrations of colistin (25, 50, and 100 µM), resulting in a final volume of 180 µL. PaβN was used as a positive control. Fluorescence measurements of Hoechst H33342 were taken every minute for 60 min at 37℃ using a Spectramax M2e (Molecular Devices) with excitation and emission wavelengths of 355 nm and 465 nm, respectively. After 5 measurements, 20 µL Hoechst H33342 was added to each well, achieving a final concentration of 2.5 µg/mL. Statistical analysis was conducted using 2-way ANOVA followed by a post-hoc Sidak test to determine the significant differences in Hoechst H33342 accumulation fluorescence between AcrB mutant and expressor strains after treatment with varying concentrations of colistin.

Ciprofloxacin accumulation by liquid chromatography/mass spectrometry (LC/MS)

Ciprofloxacin accumulation was assessed using an LC/MS-based assay following an established procedure[63]. Briefly, *K. pneumoniae* ATCC43816, *K. pneumoniae* ATCC43816_ΔacrAB::pWKS130, and *K. pneumoniae* ATCC43816_ΔacrAB::pWKS_acrAB were cultured overnight in LB medium at 37℃. Overnight cultures were diluted 50-fold and incubated at 37℃ for approximately 4 h until reaching an OD_{600} of ~ 1. Cells were washed once with 100 mM NaCl-50 mM sodium phosphate buffer (pH 7.0) and re-suspended in the same buffer at 1:10 of the original volume supplemented with 0.5% glycerol and 1% glucose. The assay was conducted in a 96-well plate with a final volume of 100 µL. Bacterial cells were pre-incubated with and without colistin (25 or 50 µM) for 10 min at 37℃, followed by the addition of ciprofloxacin (30 ng/mL) for 10 min of uptake at 37℃. Subsequently, cells were washed with ice-cold buffer and incubated with 50 µL of lysis buffer (100 mM glycine prepared in 0.1 N HCl) overnight to lyse bacterial cells. The supernatant (flow-through) was collected after centrifugation at 3275 x *g* for 5 min and used for LC/MS analysis.

For LC/MS analysis, we prepared samples and standard curves by mixing 40 µL of sample or standard, 56 µL of water, and 4 µL of internal standard (100 ng/mL levofloxacin in water). A 10 µL injection was used with a 10-minute method. The LC-MS system comprised a Shimadzu HPLC and CTC auto-sampler coupled to a PE Sciex 3000 MS. Samples were quantified by comparing with a ciprofloxacin standard curve from 1 to 32 ng/mL. Mobile phase A consisted of water with 0.1% formic acid, while mobile phase B was acetonitrile with 0.1% formic acid. Samples were separated on a C18 HPLC column (100 Å, 3 µm, 2.1 mm x 50 mm; Waters, Milford, MA, USA) heated to 40 °C using a programmed gradient of increasing mobile phase B at a flow rate of 300 µL/min. Initially, mobile phase B was increased from 5 to 20% over 5 min, followed by a ramp to 80% in 0.1 min, which was maintained for 1.9 min before returning to 5% in 0.1 min and re-equilibrating for 1.9 min. The MS operated in multiple reaction monitoring (MRM) scan mode with positive polarity. Specifically, we monitored the following MRM transitions for the analyte of interest: ciprofloxacin 332.3 > 288.3 with collision energy (CE) optimized at 25 V, and levofloxacin 362.2 > 318.3 with CE of 35 V.

Selection of resistant mutants in vitro

In our in vitro study, we prepared a suspension of *K. pneumoniae* ATCC43816 strains overexpressing AcrAB at a concentration of 10^9 CFU/mL. These bacterial suspensions were then spread onto MHA plates containing various concentrations of chloramphenicol (0.5, 1, 2, and 4 mg/L) and onto MHA plates with the same chloramphenicol concentrations supplemented with colistin (0.125, 0.25, and 0.5 mg/L). Additionally, control plates without antibiotics were included. After 48 h of incubation at 37℃, the frequency of selection of chloramphenicol-resistant mutants was determined by calculating the ratio of colonies on drug-containing plates to colonies on drug-free plates (plates without any antibiotics), as described previously[64].

Scanning electron microscopy (SEM)

SEM analysis was conducted following a standard procedure with minor adjustments[65]. In brief, *K. pneumoniae* ATCC43816 bacterial cultures in log phase (OD_{600nm} ~ 0.6) were treated with varying concentrations of colistin sulfate (12.5, 25, and 50 µM) for 30 min at 37℃. After centrifugation at 4000 rpm for 10 min, cells were washed and re-suspended in phosphate-buffered saline. Bacterial cells were fixed in 2.5% glutaraldehyde buffered with 0.15 M sodium phosphate (pH 7.0) for 1 h at room temperature. Fixed cells (100 µL) were applied to a poly-D-lysine-coated coverslip (~13 mm) in a 12-well plate and incubated at 4℃ overnight to allow bacterial cells to settle onto the coverslip. The next day, cells were washed with 0.15 M sodium phosphate buffer and treated with 1% osmium tetroxide in the same buffer for 1 h. Samples were dehydrated by passing them through graded ethanol (30%, 50%, 75%, 90%, and 100%) for 10 min at each concentration. After dehydration, samples were critical-point dried, and a thin layer of gold was spluttered onto the samples using a sputter coater system (SPI-Module™ Sputter Coater; Structure Probe Inc., West Chester, PA, USA) to prevent charging during microscopy. Bacterial cells were imaged with a Zeiss Supra 25 FESEM with Secondary, Backscatter, STEM, and EDX detectors (Carl Zeiss Microscopy, LLC, Thornwood, NY, USA).

Membrane depolarization assay

The voltage-sensitive fluorescent dye Bis (1,3-dibutylbarbituric acid) trimethine oxonol (DiBAC4(3)) (Sigma, USA) was used to evaluate changes in membrane potential of bacterial cells in the presence of colistin. DiBAC4(3) can enter depolarized cells as it binds to intracellular proteins or membranes and exhibiting enhanced fluorescence. *K. pneumoniae* overexpressing AcrAB grown to an OD600 of 0.6, washed and suspended in PBS containing 5 mM glucose. Aliquots were treated with different concentrations of colistin. After 15 min of incubation at 37℃, 0.5 µM of $DiBAC_4(3)$ a fluorescent dye was added to the bacterial suspension and incubated for another 15 min at 37℃[66]. Fluorescence at excitation and emission wavelengths of 490 nm and 516 nm were measured.

Ligand docking

Ligand docking was performed using the Glide (Grid-based Ligand Docking with Energetics) module within Schrödinger software suite (Schrodinger Release 2021-2, Schrodinger, LLC, New York, NY, 2018)[67]. The docking process involved two main steps: (1) ligand preparation and (2) protein preparation for in silico docking.

(1) ligand Preparation Prior to docking, we processed and optimized the 3-D structures of a set of potential AcrB inhibitors using the Ligprep module from the Schrodinger software suite. During ligand preparation, EPik was used to predict the pKa of the ionizable atoms within each structure, allowing us to generate structures with likely ionization and tautomerization states based on the predicted pKa values.

(2) protein Preparation and in Silico Docking The crystal structure of the AcrB membrane transport protein (PDB code 4DX5)[30] was imported into Schrodinger software suite. The protein was processed using the protein preparation wizard, excluding specific small molecules and solvent present in the structure. For in silico molecular docking studies, we utilized the Glide module within Schrodinger software suite[67,68]. The docking was centered on the MINOCYCLINE (MIY)-binding domain of the protein. Glide was run in standard precision (SP) mode, and up to five conformations of each molecule were generated and outputted prior to analysis. The docked compounds were evaluated based on their orientation and Glide/DOCK score. Additionally, we explored potential binding for colistin using the DODECYL-ALPHA-D-MALTOSIDE (LMU)-binding domain adjacent to the pocket bound by MIY in an identical fashion. The docked compounds were evaluated based on orientation and Glide score.

Binding affinity of colistin to AcrB

The binding affinity of colistin to AcrB protein was assessed using purified AcrB protein. For purification, a 3.1 kb *acrB* fragment was amplified from the genomic DNA of *K. pneumoniae* ATCC43816 strain using gene specific primers (Supplementary Table 1). The amplified fragment was cloned into pET24b plasmid and transformed into *E. coli* DH5α. The recombinant plasmid (pET24_acrB) obtained from *E. coli* DH5α was then transformed into *E. coli* DE3, and the protein was purified as previously described[69] (see supplemental methods for details). The binding parameters of colistin to AcrB were measured by isothermal titration calorimetry (ITC)[70]. The experiment was conducted with a MicroCal PEAQ-ITC (Malvern Panalytical Inc., MA) at 25 °C. The reaction sample cell was filled with 20 μM purified AcrB protein and 13 injections of 3 μL aliquots of 200 μM colistin dissolved in the same buffer (20 mM Tris Cl, pH 7.5, 50 mM sodium chloride, 0.03% DDM) were performed at 150 s intervals. The heat generated by the binding reaction was plotted versus against the colisitn/AcrB molar ratio.

Statistical analysis

All results are expressed as the mean ± SD, as indicated. Statistical analysis was performed using GraphPad Prism 6. Statistical significance between two groups was evaluated using the Student's t-test. A 2-way ANOVA followed by post-hoc Sidak test was used to determine the statistical significance between multiple groups. ($P > 0.05$ (n.s.), $^{*}P < 0.05$, $^{**}P < 0.01$, $^{***}P < 0.001$).

Data availability

The materials and reagents used are either commercially available or available upon request, with detailed information included in Methods. All data supporting the findings and materials for the manuscript are available within the article and the Supplementary Information. Please contact the corresponding author Gauri G Rao (gaurirao@usc.edu) for requests.

Received: 4 January 2025; Accepted: 28 August 2025
Published online: 03 October 2025

References

1. Nikaido, H. & Pagès, J. M. Broad-specificity efflux pumps and their role in multidrug resistance of Gram-negative bacteria. *FEMS Microbiol. Rev.* **36**, 340–363 (2012).
2. Poole, K. Efflux-mediated multiresistance in Gram-negative bacteria. *Clin. Microbiol. Infect.* **10**, 12–26 (2004).
3. Poole, K. Efflux-mediated antimicrobial resistance. *J. Antimicrob. Chemother.* **56**, 20–51 (2005).
4. Piddock, L. J. Multidrug-resistance efflux pumps? Not just for resistance. *Nat. Rev. Microbiol.* **4**, 629 (2006).
5. Abdali, N. et al. Reviving antibiotics: efflux pump inhibitors that interact with acra, a membrane fusion protein of the AcrAB-TolC multidrug efflux pump. *ACS Infect. Dis.* **3**, 89–98 (2017).
6. Sun, J., Deng, Z. & Yan, A. Bacterial multidrug efflux pumps: mechanisms, physiology and Pharmacological exploitations. *Biochem. Biophys. Res. Commun.* **453**, 254–267 (2014).
7. Lamut, A., Peterlin Mašič, L., Kikelj, D. & Tomašič, T. Efflux pump inhibitors of clinically relevant multidrug resistant bacteria. *Med. Res. Rev.* **39**, 2460–2504 (2019).
8. Padilla, E. et al. *Klebsiella pneumoniae* acrab efflux pump contributes to antimicrobial resistance and virulence. *Antimicrob. Agents Chemother.* **54**, 177–183 (2010).
9. Grimsey, E. et al. Chlorpromazine and amitriptyline are substrates and inhibitors of the AcrB multidrug efflux pump. *MBio* **11**, e00465–e00420 (2020).
10. Anes, J., McCusker, M. P., Fanning, S. & Martins, M. The Ins and outs of RND efflux pumps in *Escherichia coli*. *Front. Microbiol.* **6**, 587 (2015).
11. Oswald, C., Tam, H. K. & Pos, K. M. Transport of lipophilic carboxylates is mediated by transmembrane helix 2 in multidrug transporter AcrB. *Nat. Commun.* **7**, 1–10 (2016).
12. Pages, J. M. et al. Efflux pump, the masked side of beta-lactam resistance in *Klebsiella pneumoniae* clinical isolates. *PLoS One*. **4**, e4817–e4817 (2009).
13. Davin-Regli, A. et al. Membrane permeability and regulation of drug influx and efflux in enterobacterial pathogens. *Curr. Drug Targets*. **9**, 750–759 (2008).
14. Alibert-Franco, S. et al. Efflux pumps of gram-negative bacteria, a new target for new molecules. *Curr. Top. Med. Chem.* **10**, 1848–1857 (2010).
15. Li, X. & Nikaido, H. Efflux-mediated drug resistance in bacteria: an update. *Drugs* **69** (12), 1555–1623 (2009).
16. Wright, G. D. Antibiotic adjuvants: rescuing antibiotics from resistance. *Trends Microbiol.* **24**, 862–871 (2016).
17. Li, X. Z., Plésiat, P. & Nikaido, H. The challenge of efflux-mediated antibiotic resistance in Gram-negative bacteria. *Clin. Microbiol. Rev.* **28**, 337–418 (2015).
18. Spengler, G., Kincses, A., Gajdács, M. & Amaral, L. New roads leading to old destinations: efflux pumps as targets to reverse multidrug resistance in bacteria. *Mol* **22**, 468 (2017).
19. Wang, Y., Venter, H. & Ma, S. Efflux pump inhibitors: a novel approach to combat efflux-mediated drug resistance in bacteria. *Curr. Drug Targets*. **17**, 702–719 (2016).
20. Mazzariol, A., Zuliani, J., Cornaglia, G., Rossolini, G. M. & Fontana, R. AcrAB efflux system: expression and contribution to fluoroquinolone resistance in *Klebsiella* spp. *Antimicrob. Agents Chemother.* **46**, 3984–3986 (2002).
21. Piddock, L. J., White, D. G., Gensberg, K., Pumbwe, L. & Griggs, D. J. Evidence for an efflux pump mediating multiple antibiotic resistance in *Salmonella enterica* serovar typhimurium. *Antimicrob. Agents Chemother.* **44**, 3118–3121 (2000).
22. Poole, K. & Lomovskaya, O. Can efflux inhibitors really counter resistance? *Drug Discov Today Ther. Strateg.* **3**, 145–152 (2006).
23. Opperman, T. J. & Nguyen, S. T. Recent advances toward a molecular mechanism of efflux pump Inhibition. *Front. Microbiol.* **6**, 421 (2015).
24. Wright, G. D. Resisting resistance: new chemical strategies for battling superbugs. *Chem. Biol.* **7**, R127–R132 (2000).
25. Lomovskaya, O. et al. Identification and characterization of inhibitors of multidrug resistance efflux pumps in *Pseudomonas aeruginosa*: novel agents for combination therapy. *Antimicrob. Agents Chemother.* **45**, 105–116 (2001).
26. Kern, W. V. et al. Effect of 1-(1-naphthylmethyl)-piperazine, a novel putative efflux pump inhibitor, on antimicrobial drug susceptibility in clinical isolates of *Escherichia coli*. *J. Antimicrob. Chemother.* **57**, 339–343 (2006).
27. Yoshida, K. et al. MexAB-OprM specific efflux pump inhibitors in *Pseudomonas aeruginosa*. Part 7: highly soluble and in vivo active quaternary ammonium analogue D13-9001, a potential preclinical candidate. *Bioorg. Med. Chem.* **15**, 7087–7097 (2007).

28. Opperman, T. J. et al. Characterization of a novel Pyranopyridine inhibitor of the acrab efflux pump of *Escherichia coli*. *Antimicrob. Agents Chemother.* **58**, 722–733 (2014).
29. Lomovskaya, O. & Bostian, K. A. Practical applications and feasibility of efflux pump inhibitors in the clinic—a vision for applied use. *Biochem. Pharmacol.* **71**, 910–918 (2006).
30. Eicher, T., Cha, H. & Seeger, M. Transport of drugs by the multidrug transporter AcrB involves an access and a deep binding pocket that are separated by a switch-loop. *Proc. Natl. Acad. Sci. U S A.* **109**, 5687–5692 (2012).
31. Nikaido, H. Structure and mechanism of RND-type multidrug efflux pumps. *Adv. Enzymol. Relat. Areas Mol. Biol.* **77**, 1 (2011).
32. Piddock, L. J. Clinically relevant chromosomally encoded multidrug resistance efflux pumps in bacteria. *Clin. Microbiol. Rev.* **19**, 382–402 (2006).
33. Bhardwaj, K., Mohanty, P. & A. & Bacterial efflux pumps involved in multidrug resistance and their inhibitors: rejuvinating the antimicrobial chemotherapy. *Recent. Pat. Anti-infect Drug Discov.* **7**, 73–89 (2012).
34. Armengol, E. et al. Efficacy of combinations of colistin with other antimicrobials involves membrane fluidity and efflux machinery. *Infect. Drug Resist.* **12**, 2031–2038 (2019).
35. Abdul Rahim, N. et al. Synergistic killing of NDM-producing MDR *Klebsiella pneumoniae* by two 'old'antibiotics—polymyxin B and Chloramphenicol. *J. Antimicrob. Chemother.* **70**, 2589–2597 (2015).
36. Rudilla, H. et al. Synergistic antipseudomonal effects of synthetic peptide AMP38 and carbapenems. *Mol* **21**, 1223 (2016).
37. El Meouche, I. & Dunlop, M. J. Heterogeneity in efflux pump expression predisposes antibiotic-resistant cells to mutation. *Sci* **362**, 686–690. https://doi.org/10.1126/science.aar7981 (2018).
38. Nolivos, S. et al. Role of AcrAB-TolC multidrug efflux pump in drug-resistance acquisition by plasmid transfer. *Sci* **364**, 778–782 (2019).
39. Gifford, D. R. et al. Identifying and exploiting genes that potentiate the evolution of antibiotic resistance. *Nat. Ecoi Evol.* **2**, 1033–1039 (2018).
40. Papkou, A., Hedge, J., Kapel, N., Young, B. & MacLean, R. C. Efflux pump activity potentiates the evolution of antibiotic resistance across S. aureus isolates. *Nat. Commun.* **11**, 3970 (2020).
41. Falagas, M. E. et al. Toxicity after prolonged (more than four weeks) administration of intravenous colistin. *BMC Infect. Dis.* **5**, 1–8 (2005).
42. Akajagbor, D. S. et al. Higher incidence of acute kidney injury with intravenous colistimethate sodium compared with polymyxin B in critically ill patients at a tertiary care medical center. *Clin. Infect. Dis.* **57**, 1300–1303 (2013).
43. Pogue, J. M. et al. Incidence of and risk factors for colistin-associated nephrotoxicity in a large academic health system. *Clin. Infect. Dis.* **53**, 879–884 (2011).
44. Koch-Weser, J. et al. Adverse effects of sodium colistimethate: manifestations and specific reaction rates during 317 courses of therapy. *Ann. Intern. Med.* **72**, 857–868 (1970).
45. Falagas, M. E., Fragoulis, K. N., Kasiakou, S. K., Sermaidis, G. J. & Michalopoulos, A. Nephrotoxicity of intravenous colistin: a prospective evaluation. *Int. J. Antimicrob. Agents.* **26**, 504–507 (2005).
46. Hartzell, J. D. et al. Nephrotoxicity associated with intravenous colistin (colistimethate sodium) treatment at a tertiary care medical center. *Clin. Infect. Dis.* **48**, 1724–1728 (2009).
47. Sorlí, L. et al. Trough colistin plasma level is an independent risk factor for nephrotoxicity: a prospective observational cohort study. *BMC Infect. Dis.* **13**, 1–9 (2013).
48. Forrest, A. et al. Pharmacokinetic/toxicodynamic analysis of colistin-associated acute kidney injury in critically ill patients. *Antimicrob. Agents Chemother.* **61**, 101128aac01367–101128aac01317 (2017).
49. Horcajada, J. P. et al. Validation of a colistin plasma concentration breakpoint as a predictor of nephrotoxicity in patients treated with colistin methanesulfonate. *Int. J. Antimicrob. Agents.* **48**, 725–727 (2016).
50. Nation, R. L. et al. Dosing guidance for intravenous colistin in critically ill patients. *Clin. Infect. Dis.* **64**, 565–571 (2017).
51. Tran, T. B. et al. Pharmacokinetics/pharmacodynamics of colistin and polymyxin B: are we there yet? *Int. J. Antimicrob. Agents.* **48**, 592–597 (2016).
52. Rao, G. G. et al. New dosing strategies for an old antibiotic: pharmacodynamics of front-loaded regimens of colistin at simulated pharmacokinetics in patients with kidney or liver disease. *Antimicrob. Agents Chemother.* **58**, 1381–1388 (2014).
53. Alenazy, R. Drug efflux pump inhibitors: a promising approach to counter multidrug resistance in Gram-negative pathogens by targeting AcrB protein from AcrAB-TolC multidrug efflux pump from *Escherichia coli*. *Biol* **11**, 1328 (2022).
54. Conway, S. et al. Intravenous colistin sulphomethate in acute respiratory exacerbations in adult patients with cystic fibrosis. *Thorax* **52**, 987–993 (1997).
55. Gunderson, B. W. et al. Synergistic activity of colistin and Ceftazidime against multiantibiotic-resistant *Pseudomonas aeruginosa* in an in vitro pharmacodynamic model. *Antimicrob. Agents Chemother.* **47**, 905–909 (2003).
56. Tascini, C., Ferranti, S., Messina, F. & Menichetti, F. In vitro and in vivo synergistic activity of colistin, rifampin, and Amikacin against a multiresistant *Pseudomonas aeruginosa* isolate. *Clin. Microbiol. Infect.* **6**, 690–691 (2000).
57. CLSI. Performance standards for antimicrobial susceptibility testing; twenty-fifth informational supplement M100-S25. Clinical and Laboratory Standards Institute, Wayne, PA, (2015).
58. Huang, T. W. et al. Capsule deletion via a λ-Red knockout system perturbs biofilm formation and fimbriae expression in *Klebsiella pneumoniae* MGH 78578. *BMC Res. Notes.* **7**, 13 (2014).
59. Gust, B., Challis, G. L., Fowler, K., Kieser, T. & Chater, K. F. PCR-targeted streptomyces gene replacement identifies a protein domain needed for biosynthesis of the sesquiterpene soil odor Geosmin. *Proc. Natl. Acad. Sci. U S A.* **100**, 1541–1546. https://doi.org/10.1073/pnas.0337542100 (2003).
60. Ocaktan, A., Yoneyama, H. & Nakae, T. Use of fluorescence probes to monitor function of the subunit proteins of the MexA-MexB-OprM drug extrusion machinery in *Pseudomonas aeruginosa*. *J. Biol. Chem.* **272**, 21964–21969 (1997).
61. Paixão, L. et al. Fluorometric determination of ethidium bromide efflux kinetics in *Escherichia coli*. *J. Biol. Eng.* **3**, 1–13 (2009).
62. Richmond, G., Chua, K. L. & Piddock, L. Efflux in *Acinetobacter baumannii* can be determined by measuring accumulation of H33342 (bis-benzamide). *J. Antimicrob. Chemother.* **68**, 1594–1600 (2013).
63. Cai, H., Rose, K., Liang, L. H., Dunham, S. & Stover, C. Development of a liquid chromatography/mass spectrometry-based drug accumulation assay in *Pseudomonas aeruginosa*. *Anal. Biochem.* **385**, 321–325 (2009).
64. Drugeon, H., Juvin, M. & Bryskier, A. Relative potential for selection of fluoroquinolone-resistant *Streptococcus pneumoniae* strains by levofloxacin: comparison with ciprofloxacin, Sparfloxacin and Ofloxacin. *J. Antimicrob. Chemother.* **43**, 55–59 (1999).
65. Sharma, R. et al. Polymyxin B in combination with meropenem against carbapenemase-producing *Klebsiella pneumoniae*: pharmacodynamics and morphological changes. *Int. J. Antimicrob. Agents.* **49**, 224–232 (2017).
66. Bhattacharyya, T., Sharma, A., Akhter, J. & Pathania, R. The small molecule IITR08027 restores the antibacterial activity of fluoroquinolones against multidrug-resistant *Acinetobacter baumannii* by efflux Inhibition. *Int. J. Antimicrob. Agents.* **50**, 219–226 (2017).
67. Halgren, T. A. et al. Glide: a new approach for rapid, accurate Docking and scoring. 2. Enrichment factors in database screening. *J. Med. Chem.* **47**, 1750–1759 (2004).
68. Friesner, R. A. et al. Glide: a new approach for rapid, accurate Docking and scoring. 1. Method and assessment of Docking accuracy. *J. Med. Chem.* **47**, 1739–1749 (2004).
69. Daury, L. et al. Tripartite assembly of RND multidrug efflux pumps. *Nat. Commun.* **7**, 10731 (2016).
70. Nakashima, R. et al. Structural basis for the Inhibition of bacterial multidrug exporters. *Nat* **500**, 102 (2013).

Acknowledgements
G.G.R., and T.V. are supported by the National Institute of Allergy and Infectious Diseases, award number R01AI146241. The content is solely the responsibility of the authors and does not necessarily represent the official views of the National Institutes of Health. We thank the staff at the Center of Excellence in NanoBiophysics at the University of Southern California for assistance in performing ITC data collection and analysis.

Author contributions
RS and GGR designed the experiments, RS performed experiments and analyzed the data, RS and GGR wrote the manuscript, TV, BB, LH edited, LH designed intracellular measurement. VC performed the ligand docking.

Declarations

Competing interests
The authors declare no competing interests.

Additional information
Correspondence and requests for materials should be addressed to G.G.R.

Reprints and permissions information is available at www.nature.com/reprints.

Publisher's note Springer Nature remains neutral with regard to jurisdictional claims in published maps and institutional affiliations.